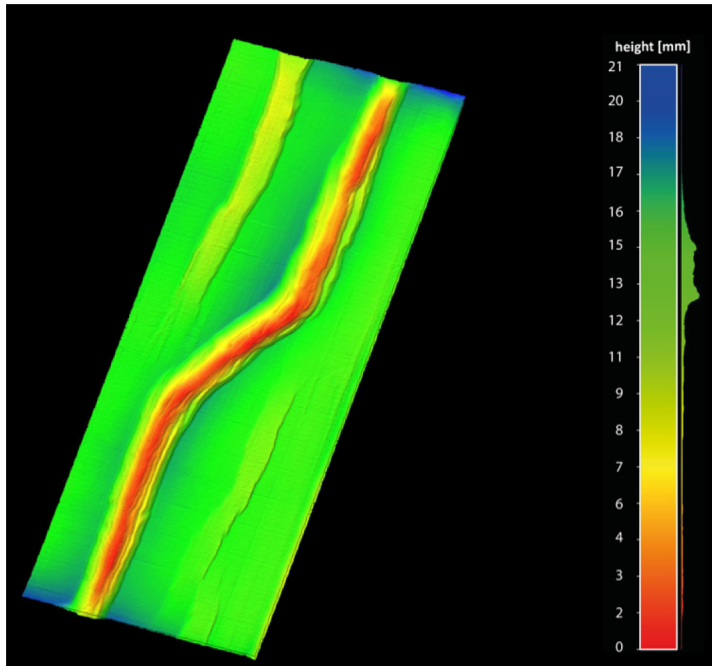


# The role of tectonic inheritance in multiphase rifting: Insights from analogue model experiments

Guido Schreurs & Mario Böhler



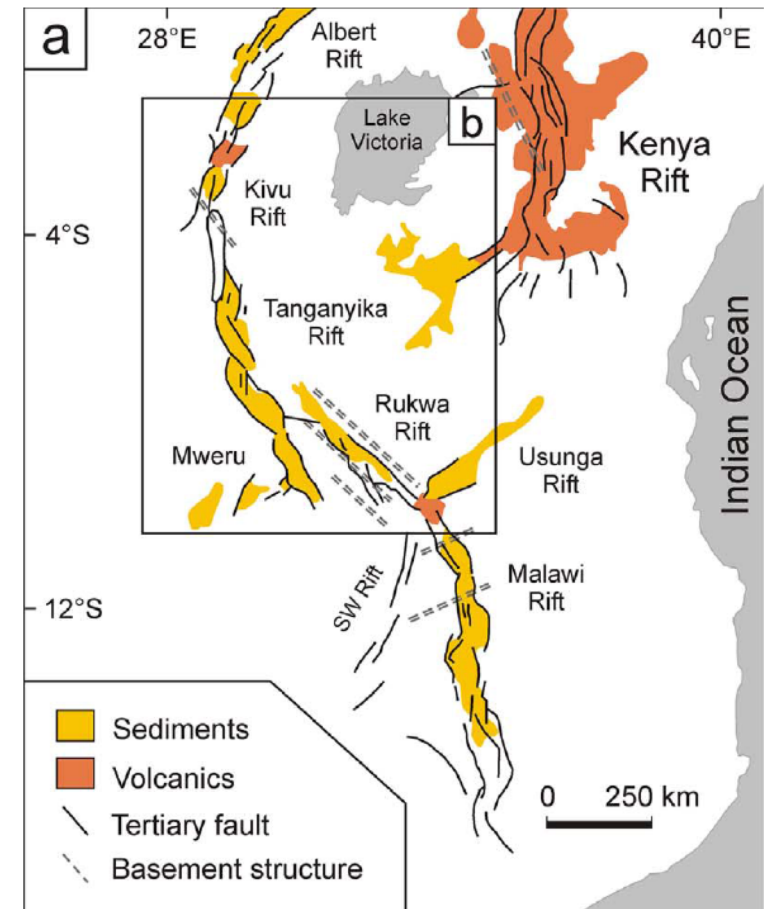
## Motivation

### Observations in nature:

- Non-linear weakness zones are common in the crust and mantle
- Rift formation is often influenced by inherited weaknesses
- Many rifts are the results of more than one phase of rifting

### Aims of this study:

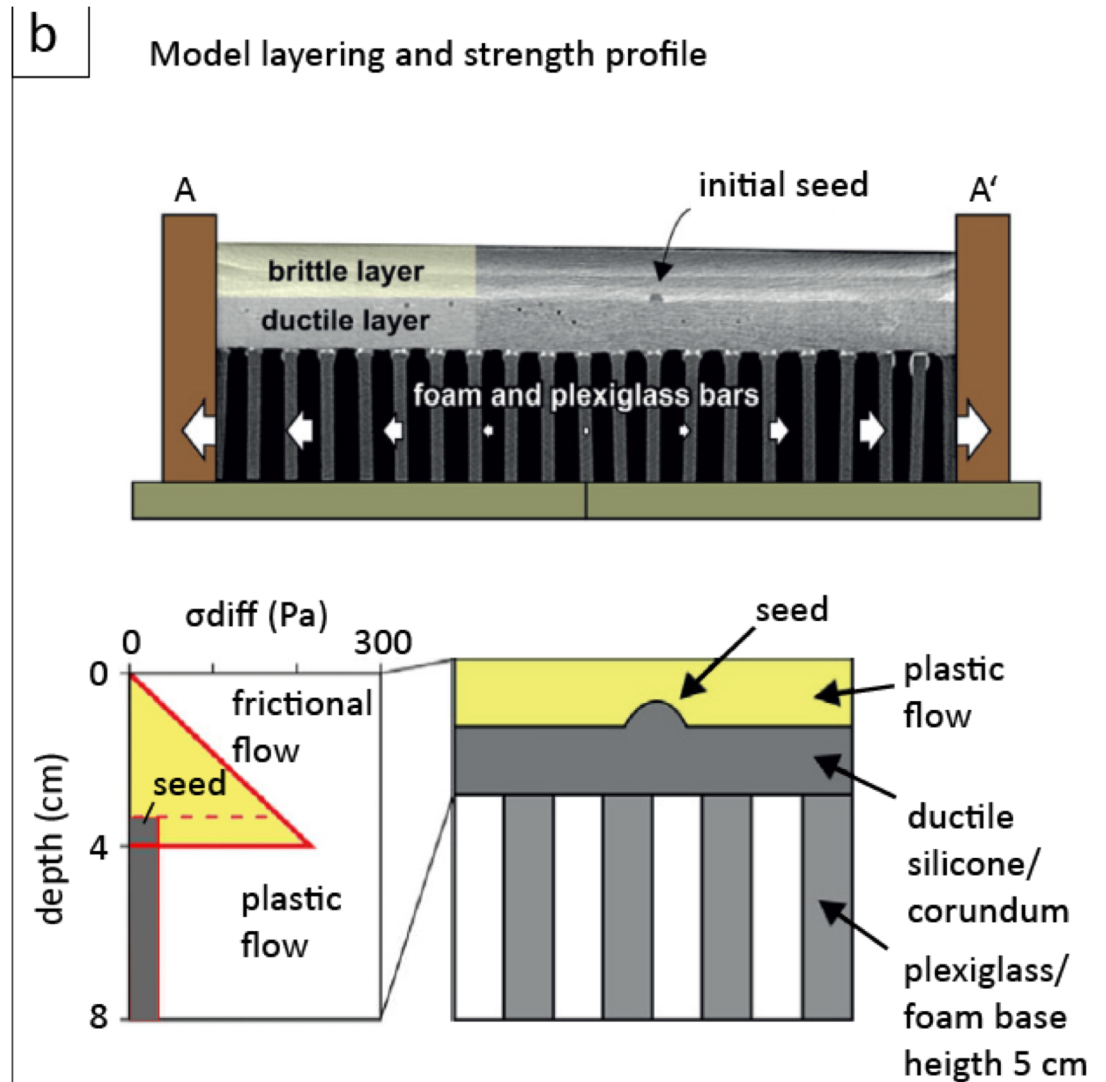
- To study the influence of a non-linear crustal weakness on rift formation
- To subsequently investigate how a first-phase rift is modified by a second phase of non-coaxial rifting



East African Rift System © Zwaan et al., 2018

## Analogue model materials

- Brittle quartz sand layer overlying a viscous layer
- Viscous seed simulates inherited weakness
- Plexiglass/foam base is compressed before model construction and allows orthogonal and oblique extensional movements of overlying model



# Analogue model materials

Physical characteristics and mechanical properties of:

- Quartz sand
- Viscous material (mixture of polydimethylsiloxane and corundum sand)

Granular material	Quartz sand												
Grain size distribution (wt %)	<table border="1"> <caption>Grain size distribution data (estimated from chart)</caption> <thead> <tr> <th>Grain size (µm)</th> <th>Percentage (%)</th> </tr> </thead> <tbody> <tr> <td>&lt;061</td> <td>0</td> </tr> <tr> <td>061-088</td> <td>15</td> </tr> <tr> <td>088-125</td> <td>0</td> </tr> <tr> <td>125-175</td> <td>65</td> </tr> <tr> <td>175-250</td> <td>15</td> </tr> </tbody> </table>	Grain size (µm)	Percentage (%)	<061	0	061-088	15	088-125	0	125-175	65	175-250	15
Grain size (µm)	Percentage (%)												
<061	0												
061-088	15												
088-125	0												
125-175	65												
175-250	15												
Grain shape <sup>1</sup>	<ul style="list-style-type: none"> <li>• Roundness: angular</li> <li>• Sphericity: low</li> </ul>												
Density (sieved)	1560 kg/m <sup>3</sup>												
Coefficient of internal peak friction	0.73												
Coefficient of dynamic-stable friction	0.61												
Angle of internal peak friction	36.1°												
Angle of dynamic-stable friction	31.4°												
Strain softening <sup>2</sup>	16%												
Cohesion	9 ± 98 Pa												
Viscous Material	PDMS/corundum sand mixture												
Weight ratio PDMS : corundum sand	0.965 kg: 1.00 Kg												
Mixture density	Ca. 1600 kg/m <sup>3</sup>												
Viscosity <sup>3</sup>	Ca. 1.5 · 10 <sup>5</sup> Pa s												
Type	Near-Newtonian (n = 1.05) <sup>4</sup>												

Brittle layer

Ductile layer

<sup>1</sup> Grain shape determined after Powers (1953)

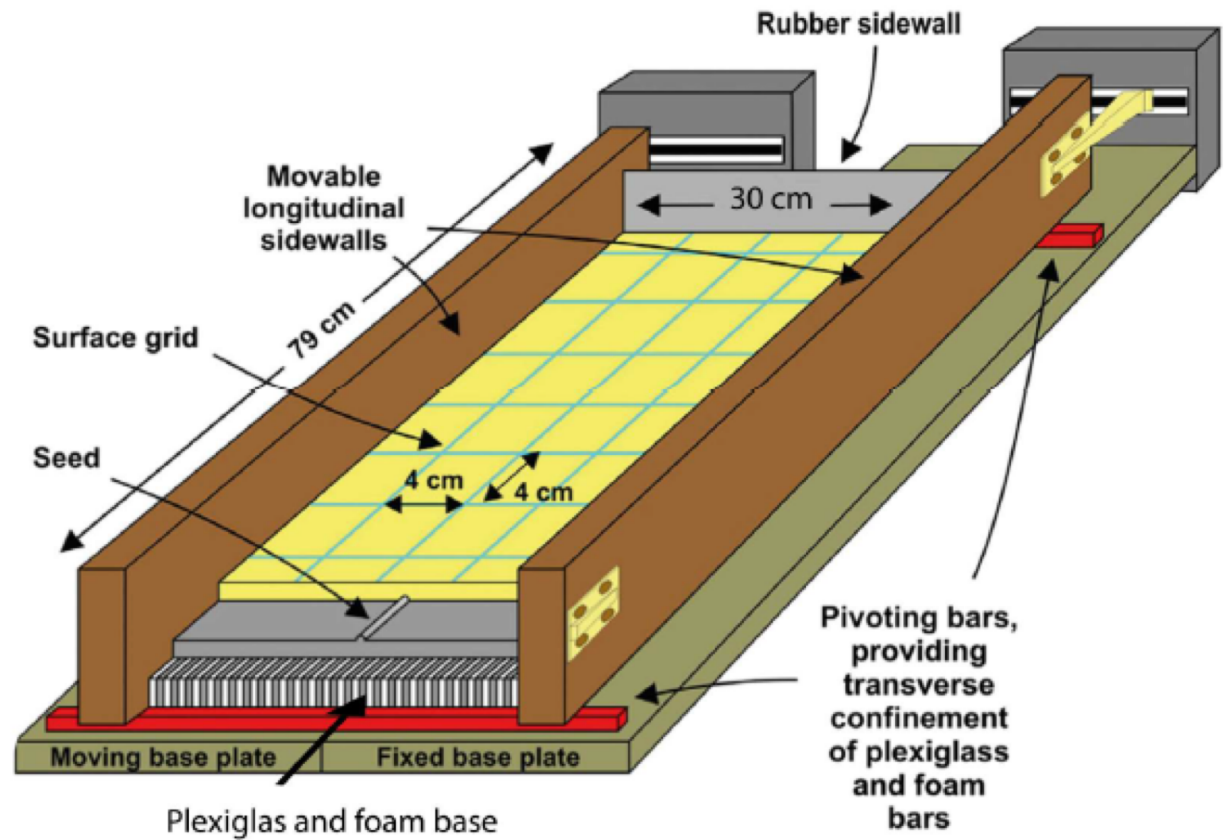
<sup>2</sup> Strain softening is the difference between peak strength and dynamic-stable strength, divided by peak strength.

<sup>3</sup> Viscosity value holds for model strain rates < 10<sup>5</sup> s<sup>-1</sup>

<sup>4</sup> Stress exponent n (dimensionless) represents sensitivity to strain rate.

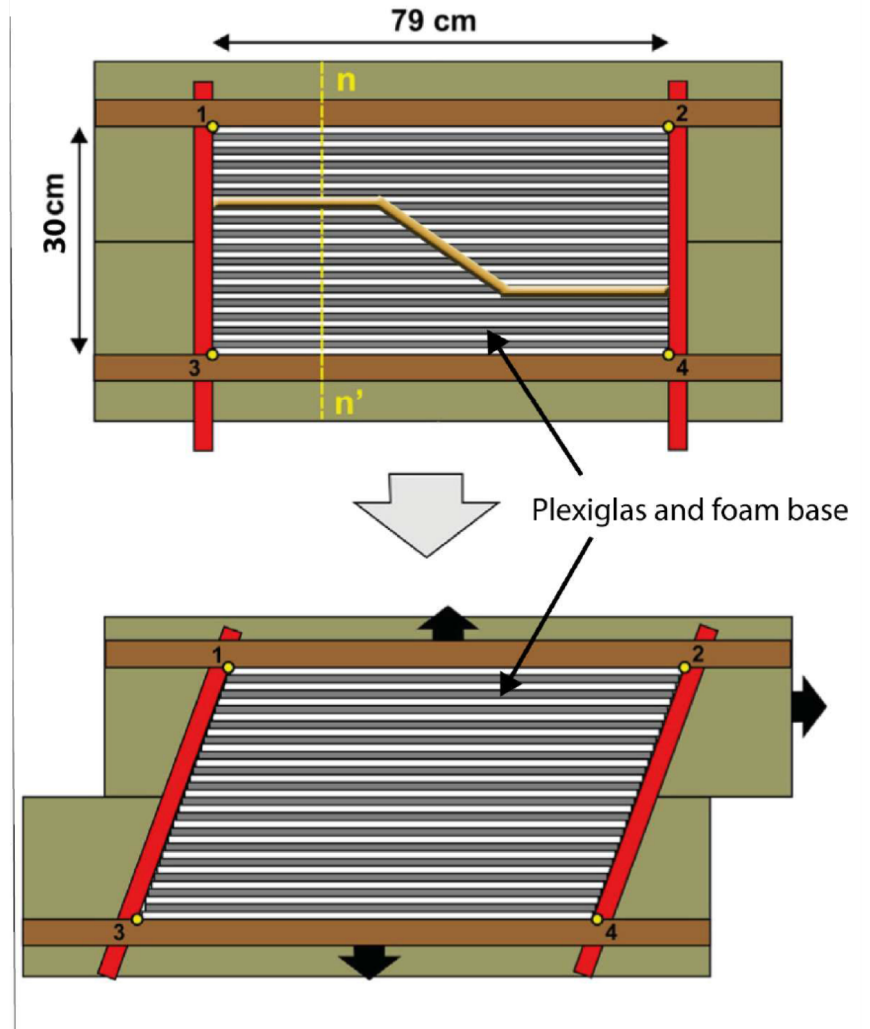
## Analogue model set-up

- Initial model dimensions: 79 x 30 cm
- 2 cm of brittle quartz sand
- 2 cm of viscous silicone/corundum sand mixture



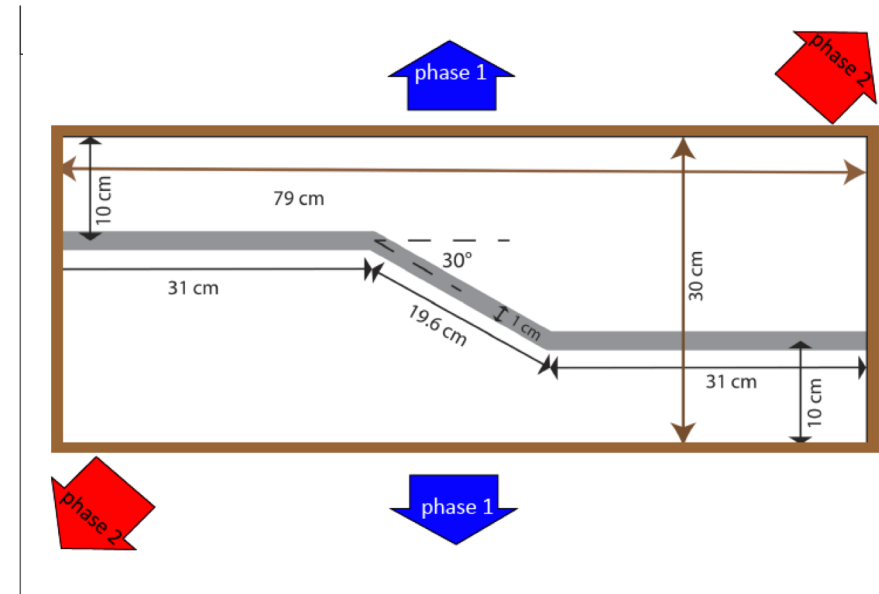
## Analogue model – basal set-up

- Initial rectangular model becomes a parallelogram during oblique extension
- Oblique extension consists of an outward movement of the longitudinal walls combined with a lateral movement of one of the base plates

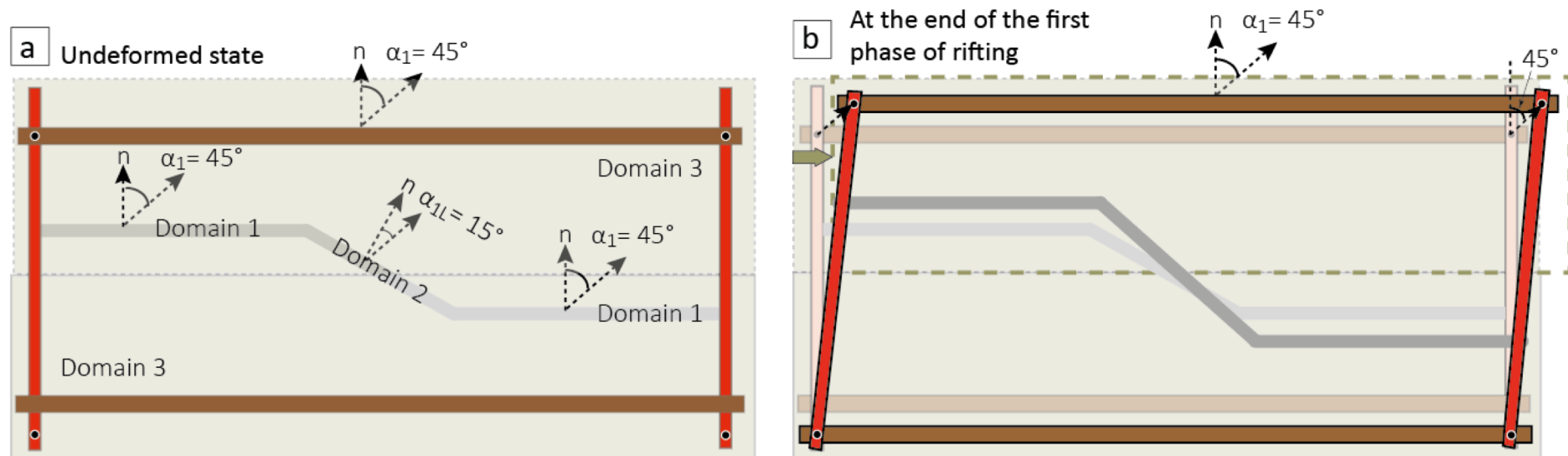


## Analogue model - seed

- Non-linear viscous seed consists of two parallel segments connected by a oblique central segment
- Dark grey line shows initial position of viscous seed. Blue and red arrows indicate an example of orientations of first and second phase of rifting
- All models undergo two phases of rifting: either a first-phase orthogonal rifting followed by a second phase of oblique rifting or vice versa



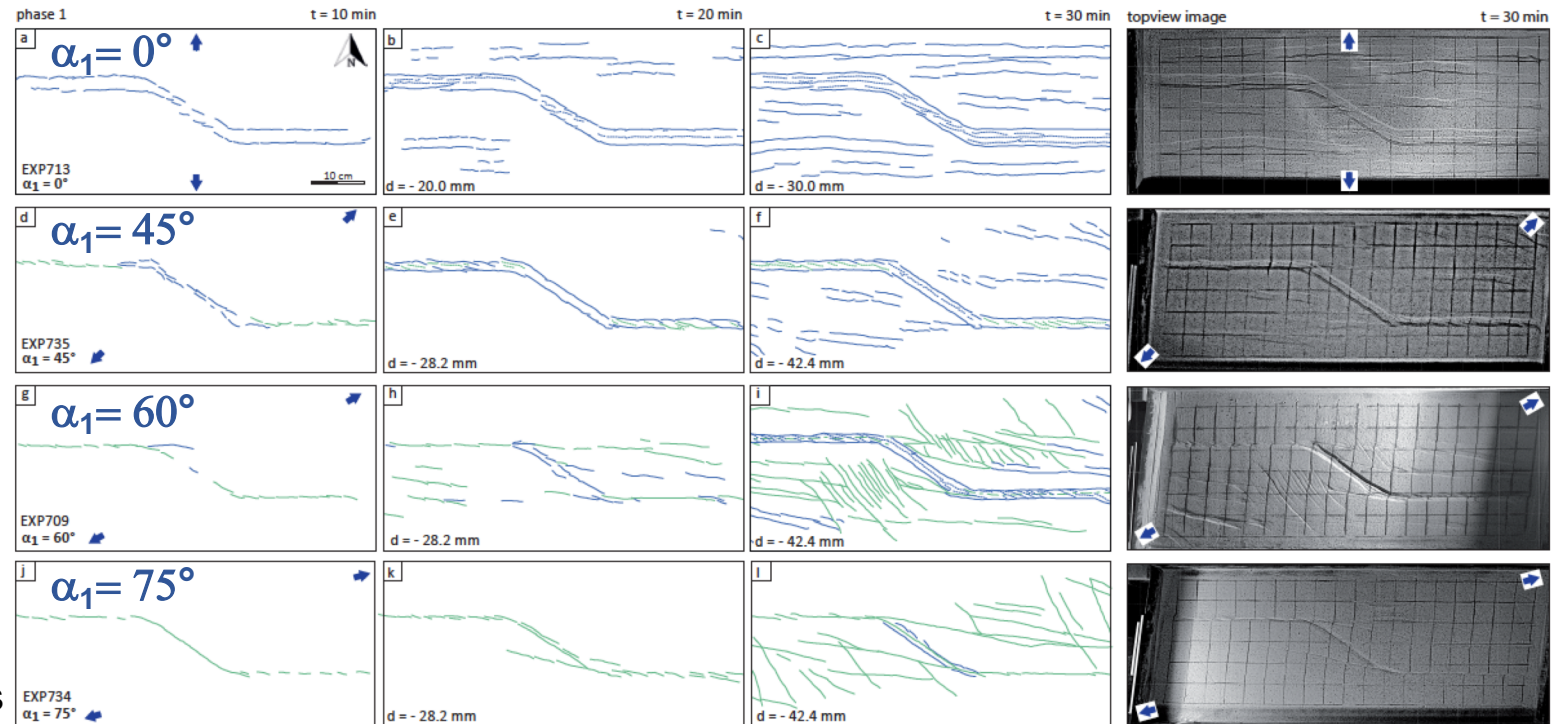
## Definition of regional ( $\alpha_1$ ) and local rift obliquity ( $\alpha_{1L}$ )



- We define three model domains: **domain 1** (E-W segments of seed), **domain 2** (oblique seed segment, striking at N120°E), **domain 3** (remainder of model)
- Regional (bulk) obliquity of first-phase rifting ( $\alpha_1$ ) in this example is 45°, whereas local rift obliquity ( $\alpha_{1L}$ ) for oblique segment (domain 2) is 15°
- Note that dextral oblique extension results in a slight clockwise rotation of domain 2

# Model results at the end of the first phase of rifting: fault evolution as a function of first-phase rift obliquity ( $\alpha_1$ )

- Faults initially localize above crustal weakness (seed); distributed faulting away from seed with time
- Early faulting: switch from dip-slip dominated normal faults (blue) to strike-slip dominated faults (green) with increasing first-phase rift obliquity angle
- At end of the first phase a major rift („master rift“) has formed above the entire length of the seed, except for  $\alpha_1 = 75^\circ$

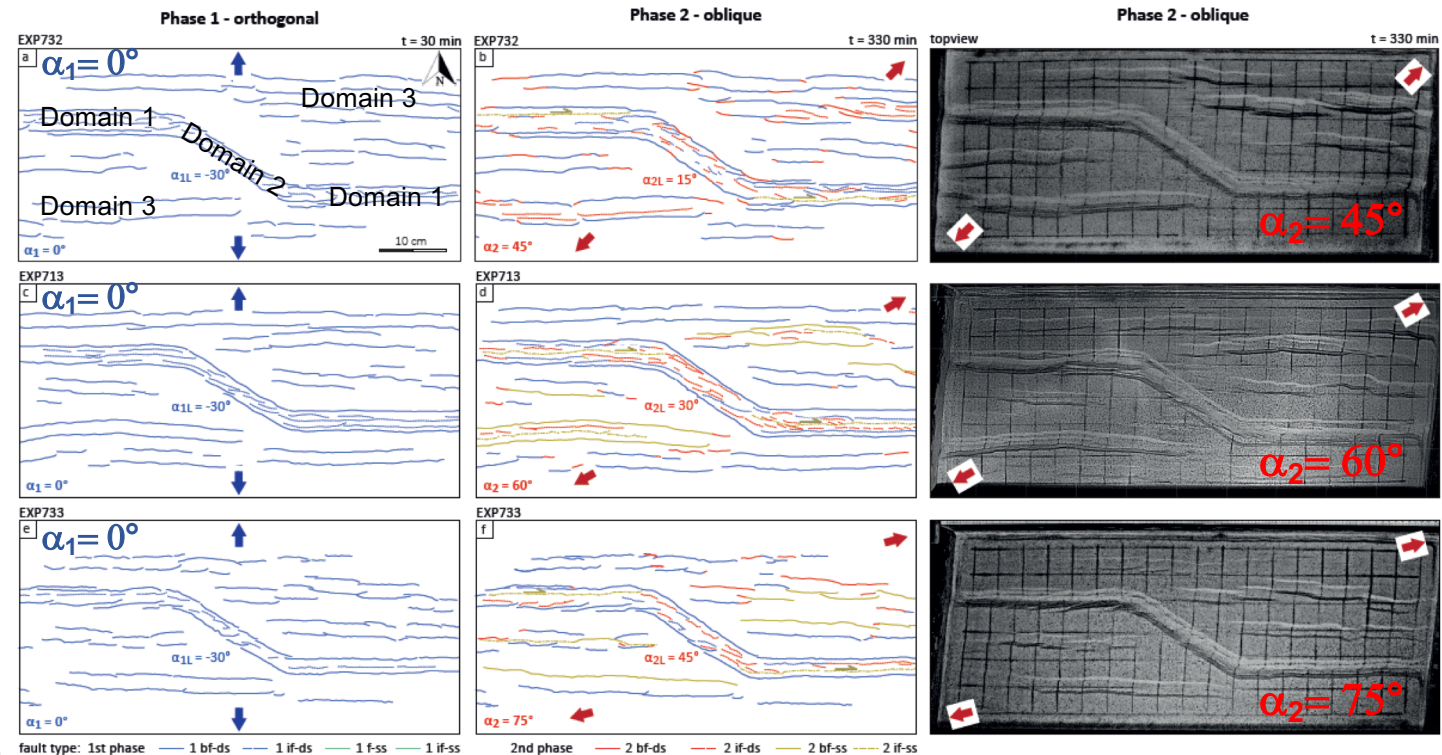


**fault type** 1st phase — 1 bf-ds — 1 f-ss  
 - - - 1 if-ds - - - 1 if-ss

- bf = boundary fault; if = intra-rift fault; f = fault
- ds = dip-slip dominated, ss = strike-slip dominated

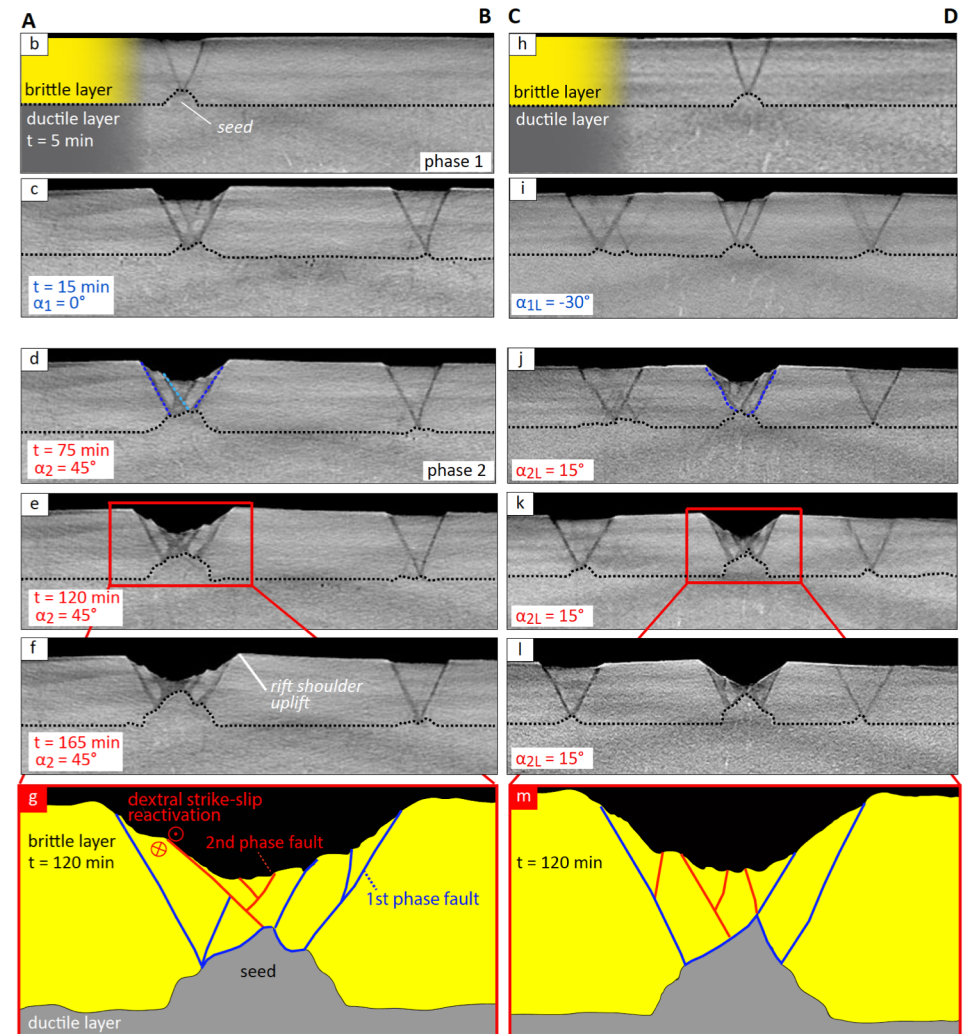
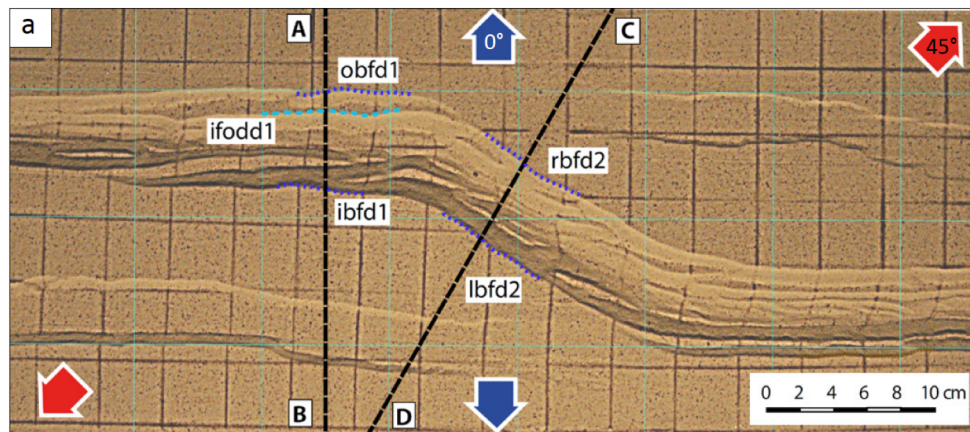
## Model results: orthogonal rifting ( $\alpha_1 = 0^\circ$ ) followed by oblique rifting ( $\alpha_2 = 45^\circ$ , $60^\circ$ or $75^\circ$ )

- The second phase of rifting results in wider and deeper rifts, mostly by formation of new intra-rift faults.
- First-phase rift-boundary faults of master rift (domain 1 and 2) remain largely inactive
- Second phase of rifting results in dextral reactivation of normal faults (orange) in domains 1 and 3 and in new (intra-rift) normal faults (red), which are short and en echelon in domain 2, striking at an angle to the rift boundary faults



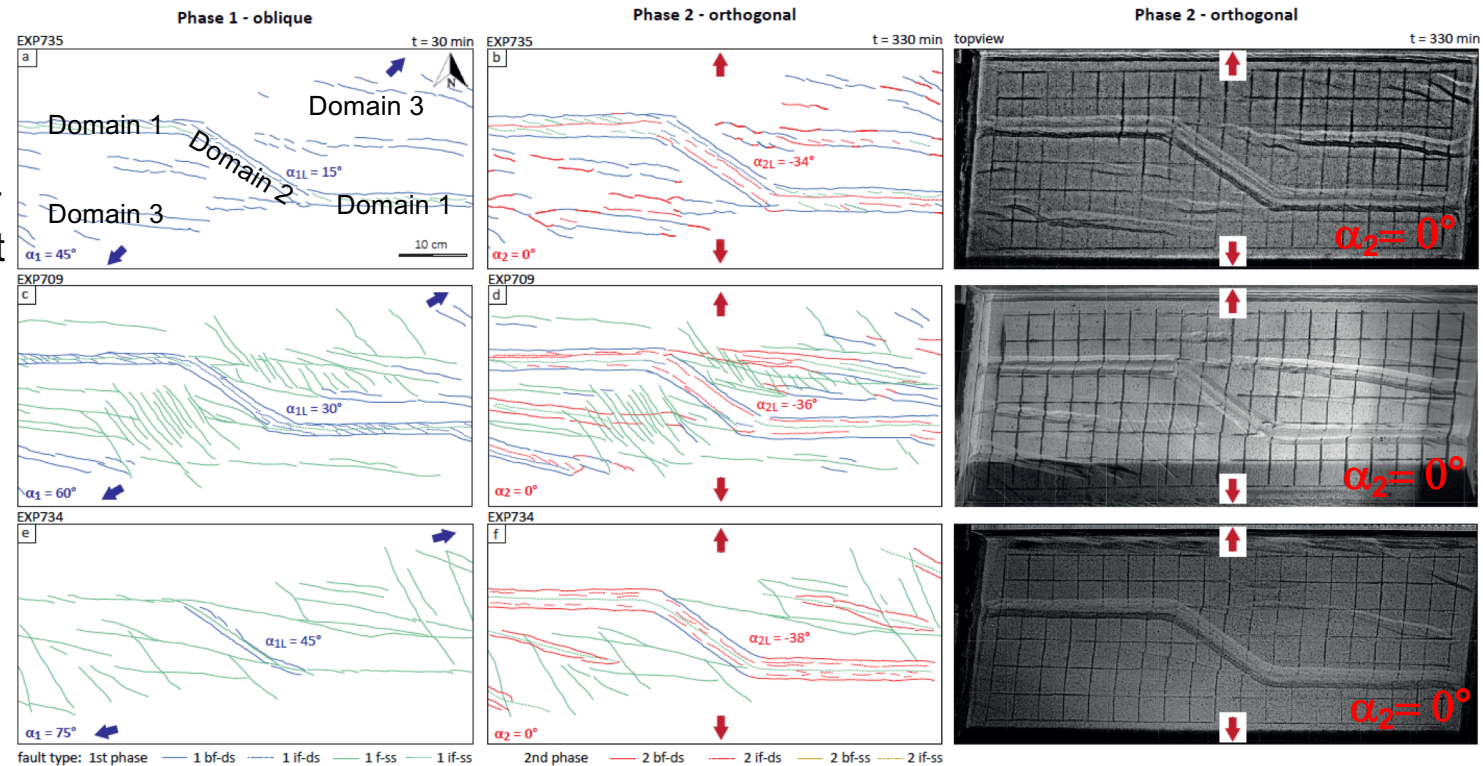
## Model results: orthogonal rifting ( $\alpha_1 = 0^\circ$ ) followed by oblique rifting ( $\alpha_2 = 45^\circ$ )

- Surface view (below) and X-ray CT cross-sections (right)
- First-phase intra-rift normal faults in E-W segments of master rift (sections A-B) acquire a dextral strike-slip component during second-phase oblique rifting ( $\alpha_2 = 45^\circ$ ), whereas new intra-rift normal faults form in the central oblique segment of the master rift (sections C-D)



# Model results: oblique rifting ( $\alpha_1 = 45^\circ, 60^\circ$ or $75^\circ$ ) followed by orthogonal rifting ( $\alpha_2 = 0^\circ$ )

- The second phase of rifting results in wider and deeper rifts, mostly by formation of new intra-rift faults (except for  $\alpha_1 = 75^\circ$ , where a rift does not form in domain 1 until the second phase of rifting)
- Second phase intra-rift faults are predominantly dip-slip dominated normal faults, which are rather long and strike parallel to the main rift boundary faults in domain 1 and 2



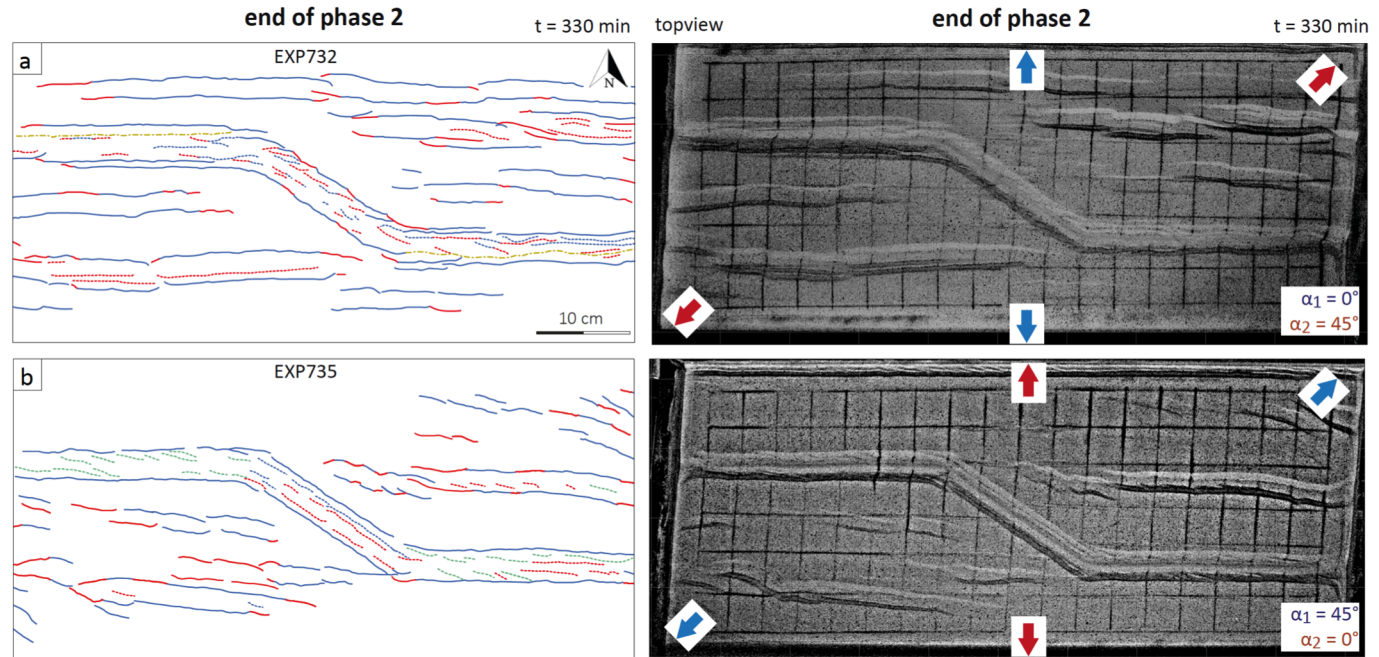
# Comparison: relative order of two-phase non-coaxial rifting is switched

- First row:  $\alpha_1 = 0^\circ$ ,  $\alpha_2 = 45^\circ$
- Second row:  $\alpha_1 = 45^\circ$ ,  $\alpha_2 = 0^\circ$

• Figures show models at the end of the second phase of rifting

• Final geometry of master rift (domains 1 and 2) looks quite similar at first glance, despite very different multiphase rifting history (but differences do occur when looking in detail)

• Note difference in strike of first-phase normal faults in domain 3, reflecting difference in first-phase obliquity

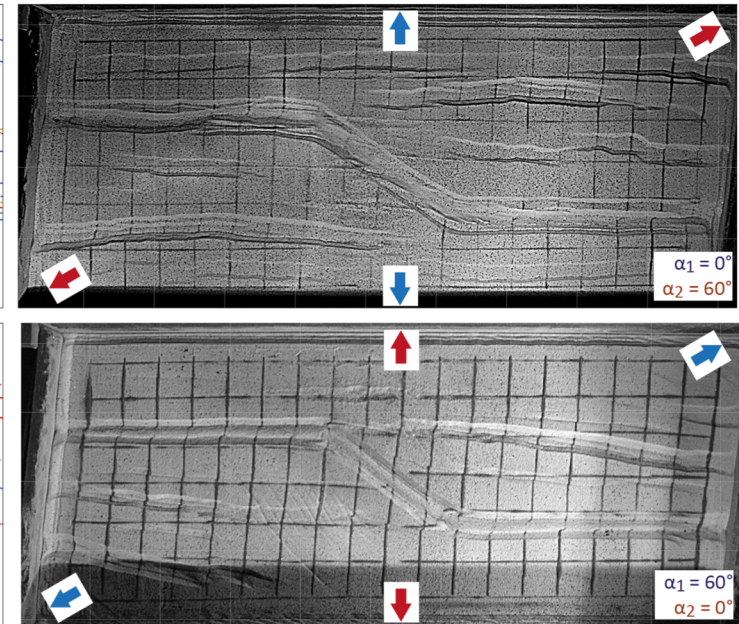
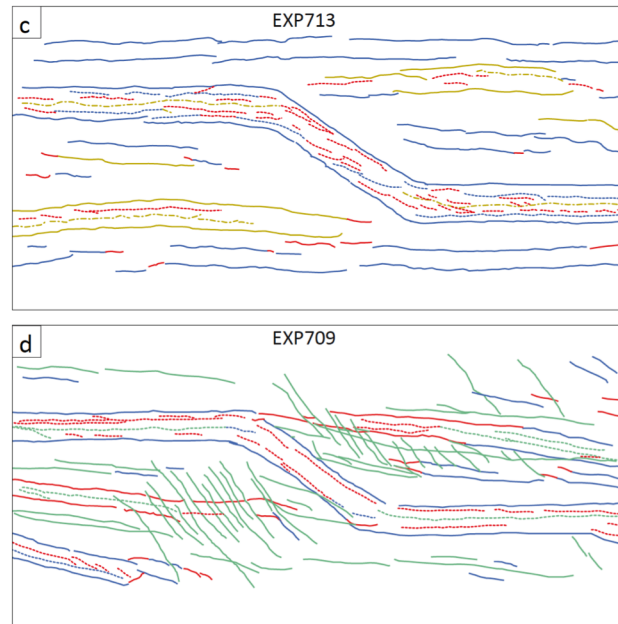


fault type 1st phase — 1 bf-ds — 1 f-ss 2nd phase — 2 bf-ds — 2 bf-ss  
 — 1 if-ds — 1 if-ss — 2 if-ds — 2 if-ss

- bf = boundary fault; if = intra-rift fault; f = fault
- ds = dip-slip dominated, ss = strike-slip dominated

## Comparison: relative order of two-phase non-coaxial rifting is switched

- First row:  $\alpha_1 = 0^\circ$ ,  $\alpha_2 = 60^\circ$
- Second row:  $\alpha_1 = 60^\circ$ ,  $\alpha_2 = 0^\circ$
- Figures show models at the end of the second phase of rifting
- Final geometry of the master rift (domains 1 and 2) looks quite similar at first glance, despite very different multiphase rifting history (but differences do occur)
- Note presence of first-phase sinistral and dextral strike-slip faults in domain 3, reflecting difference in first-phase obliquity



**fault type** 1st phase — 1 bf-ds — 1 f-ss 2nd phase — 2 bf-ds — 2 bf-ss  
 — 1 if-ds — 1 if-ss — 2 if-ds — 2 if-ss

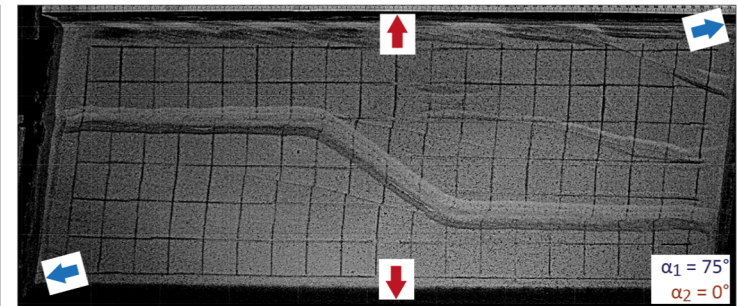
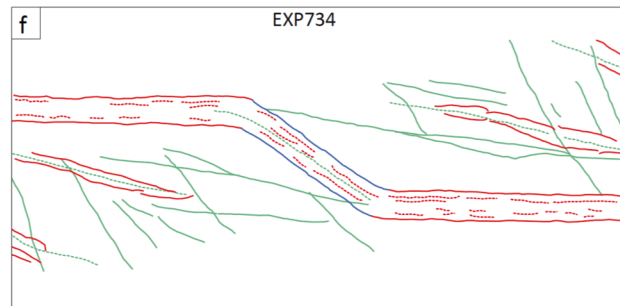
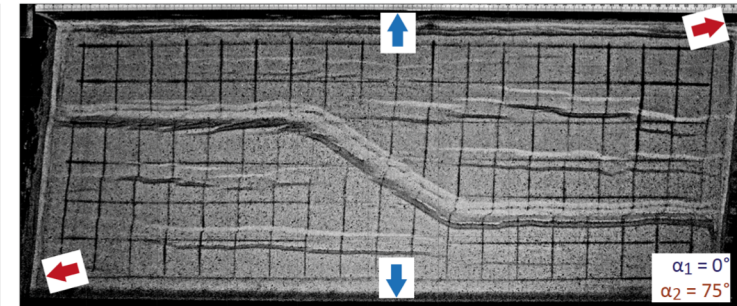
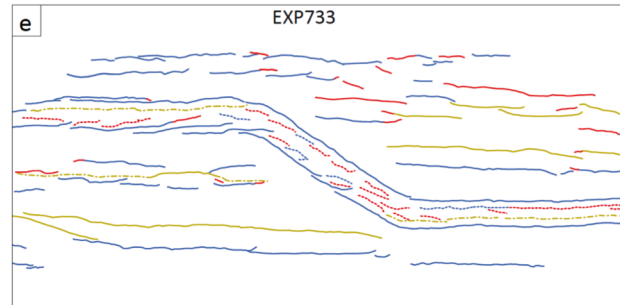
- bf = boundary fault; if = intra-rift fault; f = fault
- ds = dip-slip dominated, ss = strike-slip dominated

# Comparison: relative order of two-phase non-coaxial rifting is switched

- First row:  $\alpha_1 = 0^\circ$ ,  $\alpha_2 = 75^\circ$
- Second row:  $\alpha_1 = 75^\circ$ ,  $\alpha_2 = 0^\circ$

- Figures show models at the end of the second phase of rifting

- Final geometry of master rift (domains 1 and 2) looks quite similar, despite very different multiphase rifting history (but differences do occur)



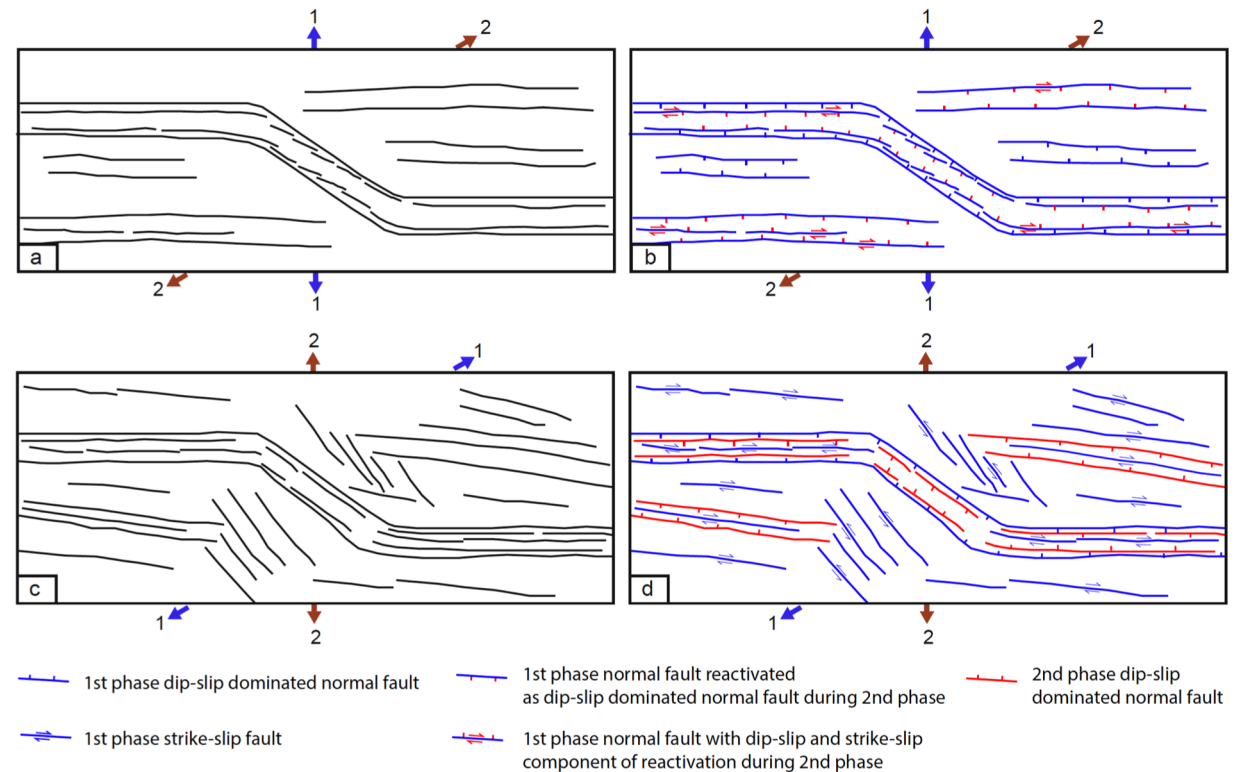
- Note presence of sinistral and dextral strike-slip faults in domain 3, reflecting difference in first-phase obliquity

**fault type** 1st phase — 1 bf-ds — 1 f-ss 2nd phase — 2 bf-ds — 2 bf-ss  
 — 1 if-ds — 1 if-ss — 2 if-ds — 2 if-ss

- bf = boundary fault; if = intra-rift fault; f = fault
- ds = dip-slip dominated, ss = strike-slip dominated

## Schematic figure showing influence of relative order of rifting in models with a pre-existing crustal weakness

- Despite the fact that the crustal weakness exerts an important control on the overall orientation of the master rift, the nature and orientation of faults both within the master rift and away from it, allow to infer the relative order of non-coaxial rifting
- (a-b) Model that has undergone first-phase orthogonal rifting and second-phase oblique rifting
- (c-d) Model that has undergone first-phase oblique rifting and second-phase orthogonal rifting



## Main conclusions – 1

- The inherited, non-linear crustal weakness has a strong influence on the localisation, nature and orientation of faulting during two phases of non-coaxial rifting, ultimately producing a master rift that mimics the orientation of the underlying weakness.
- Although the overall geometry of the master rift looks at first glance quite similar for very different rift histories (underlining the strong control of the crustal weakness), close inspection of the master rift reveals differences depending on the relative order of the two phases of non-coaxial rifting.
- Oblique rifting overprinting orthogonal rifting results in strike-slip reactivation of first phase intra-rift normal faults and short en-echelon intra-rift normal faults above the oblique segment of the tectonic inheritance, striking slightly oblique to the rift-boundary faults, (ii) orthogonal rifting superposed on oblique rifting on the other hand results in the preservation of long, first phase strike-slip faults trending parallel to later formed rift-boundary faults and parallel striking intra-rift normal faults.

## Main conclusions – 2

- First-phase structures away from the master rift (and the inherited crustal weakness) have more freedom to evolve in response to the regional extension and although these structures may be reactivated during the second phase of non-coaxial rifting, their nature and orientation at the end of the second phase reflects whether first-phase rifting was orthogonal or oblique.
- Our analogue models can be used to assess the influence of pre-existing, inherited structures on faulting in natural settings that have undergone either single-phase (oblique or orthogonal) rifting or two phase non-coaxial rifting. Furthermore, in case of natural settings where two rift phases are suspected, our model experiments can help in establishing the relative order of rifting and the relative difference in rift obliquity.